

Review

Application in Nanomedicine of Manganese-Zinc Ferrite Nanoparticles

Laura Maria Slavu¹, Rosaria Rinaldi^{1,2,3} and Riccardo Di Corato^{2,*} 

¹ Mathematics and Physics “E. De Giorgi” Department, University of Salento, Via Monteroni, 73100 Lecce, Italy; lauramaria.slavu@unisalento.it (L.M.S.); rosaria.rinaldi@unisalento.it (R.R.)

² Institute for Microelectronics and Microsystems (IMM), CNR, Via Monteroni, 73100 Lecce, Italy

³ Scuola Superiore ISUFI, University of Salento, Campus Ecotekne, Via Monteroni, 73100 Lecce, Italy

* Correspondence: riccardo.dicorato@cnr.it

Abstract: Besides the study and the medical application of iron oxide nanoparticles, ferrites produced with zinc and manganese are of particular interest for their properties. The introduction of these elements into the crystalline structure of the magnetic particle generates some changes in the material properties, enhancing their potential use in theranostic applications. This review will cover the most important aspects of the preparation of these materials, taking into account the different methods of synthesis, and will analyze the most promising results in their use in MRI, magnetic hyperthermia and other emerging applications.

Keywords: magnetic nanoparticles; Mn-Zn ferrites; nanomedicine; MRI; magnetic hyperthermia



Citation: Slavu, L.M.; Rinaldi, R.; Di Corato, R. Application in Nanomedicine of Manganese-Zinc Ferrite Nanoparticles. *Appl. Sci.* **2021**, *11*, 11183. <https://doi.org/10.3390/app112311183>

Academic Editor: Costica Caizer

Received: 7 November 2021

Accepted: 23 November 2021

Published: 25 November 2021

Publisher's Note: MDPI stays neutral with regard to jurisdictional claims in published maps and institutional affiliations.



Copyright: © 2021 by the authors. Licensee MDPI, Basel, Switzerland. This article is an open access article distributed under the terms and conditions of the Creative Commons Attribution (CC BY) license (<https://creativecommons.org/licenses/by/4.0/>).

1. Introduction

Over the past years, the field of nanotechnology has exploited the improved novel physical, chemical and biological properties of materials at the nanometric scale. Nowadays, nanomedicine has great future opportunities that aim to provide site-specific therapeutics with reduced adverse effects, novel imaging methods for diagnosis and novel implant materials that support tissue regeneration processes [1]. The use of engineered nanomaterials promotes the development of new highly effective methods for diagnostics and cancer therapy [2].

Within this framework, magnetic nanoparticles (MNPs) play an important role because of their unique characteristics and properties [3]. Nanoparticles (NPs) with high surface volume can be synthesized with a size compatible with biological molecules such as protein or nucleic acid and with unique physical and chemical properties, like high magnetic permeability, low core loss, high-permeability and optical low-power losses [4]. One of the most important properties of the magnetic nanoparticles is their superparamagnetic behavior which has aroused a very high interest in nanomedicine due to its crystalline size, which is smaller than 20 nm. In this case, each nanoparticle becomes a single magnetic domain and shows superparamagnetic behavior with a large constant magnetic moment [5]. In nanomedicine, magnetic nanoparticles have been exploited in intracellular magnetic hyperthermia, in novel photothermic treatments, in magnetic resonance imaging (MRI), in Magnetic Particle Imaging (MPI), in magnetic-guided drug delivery, in integrated biosensors and in bio-separations [6,7].

In the class of the magnetic nanomaterials, the doped ferrites nanoparticles arose a particular interest in the community. A suitable amount of an addition of zinc, manganese, cobalt or nickel to the ferrite nucleus of the NPs results in a higher magnetic resonance imaging contrast and an increase of saturation magnetization (Ms), which can lead to more efficient magnetic targeting [8]. Therefore, by adjusting their ratio cations in the unit cell, the crystal structure and properties of the ferrites can be tuned, which allows it to serve as

an ideal system for investigating the cation interaction in spinel ferrites and the influence of cation distribution on their magnetic properties [9].

Concerning magnetic hyperthermia, high values of the specific absorption rate (SAR) are required for generating an adequate temperature increase, which is achieved by keeping the amount of the nanoparticles administered as low as possible [10,11]. To enhance the SAR, different aspects were evaluated, as composition, shape or structure. Different studies have proven that the introduction of Mn and Zn in the magnetic nanoparticle structure, which optimizes the nanoparticle composition, induces higher SAR values in comparison to other doping elements, such as nickel or cobalt [12,13]. Furthermore, the magnetic properties of the Mn-Zn ferrites, (i.e., saturation magnetization and magnetic susceptibility) can be tuned and controlled by altering the composition of the material. The initial studies on this soft magnetic material were entirely focused on magneto-electronics device applications [14]. Only in the last 10–15 years has the scientific community started to use this sub-class of ferrites in nanomedicine.

This review will focus on the applications of Mn-Zn ferrite NPs in biomedical applications, by covering the most important aspects of the preparation of these materials, the different methods of synthesizing and summarizing the most promising results in their use in MRI, magnetic hyperthermia and other emerging applications in the field of nanomedicine.

2. Synthetic Strategies of Mn-Zn Ferrites

There are different preparation techniques for the synthesis of ferrite nanoparticles that exhibit novel properties which are dependent on their structural characteristics, like particle size and shape. Various methods, described below, such as co-precipitation, thermal decomposition, hydrothermal methods and sol-gel, are used to prepare spinel manganese-zinc ferrite nanocrystals.

2.1. Co-Precipitation Method

The co-precipitation method is one of the most utilized synthesis methods for preparing magnetic nanoparticles [15]. The formation of magnetic nanoparticles is due to the nucleation followed by the crystal growth and there are two steps to follow this precipitation process [16]. The first step is to take account of the solubility for each type of solute and the second step is the addition of an excess of solute, which could result in the precipitation and formation of nanocrystals. For example, for the formation of nanoparticles, the solution has to be in a high state of saturation to start the nucleation. In this case, two kinds of nucleation processes could occur: the heterogeneous nucleation (when nuclei collide and interact with a solid surface) and homogenous nucleation (which takes place in the absence of a solid interface by combining solute molecules to produce nuclei) [17]. Furthermore, for having a uniformity of particle size, it is necessary for distribution to follow a short nucleation period in such a way so as to obtain the uniformity of the nanoparticles without further nucleation. As such, the burst nucleation (induction of a single event) is obtained by increasing the concentration of metal precursors to the critical saturation point. Their magnetization depends on different parameters, like the pH of the suspension, the reaction temperature, and the initial molar concentration [18,19]. The major drawback of the co-precipitation method is the insufficient size control distribution and the uncontrolled shape, but, nonetheless, this process is a favored route to produce magnetic nanoparticles due to it requiring a low reaction temperature, the high reaction yield and the shorter reaction time than other methods, such as thermal decomposition or hydrothermal synthesis.

Most of the articles concerning the synthesis of Mn-Zn ferrite NPs exploited the synthesis by co-precipitation. Mainly iron, zinc and manganese chlorides are used [20–25], but also the respective nitrates [26,27] and sulfates [28,29] have been used in various articles. The principle of synthesis is almost always identical and involves the preparation of an aqueous solution of three metal salts and the subsequent addition of a base (mainly NaOH, but also ammonium hydroxide) to induce the co-precipitation of the magnetic nanoparticles. Several studies focused on the analysis of the composition of the nanoparticle, studying the

relationship between Mn and Zn in the typical formula $Mn_{(1-x)}Zn_xFe_2O_4$, related to the typical spinel structure found in this type of nanoparticles. A linear trend was not observed in the literature, as for some studies an increase in the Ms is obtained by increasing the percentage of zinc [20,26], while for others it is the increase of manganese [27,29] that determines a greater Ms. In general, it can be claimed that an equal ratio between the elements (0.5 Mn/0.5 Zn) [24] or a ratio that is slightly shifted towards manganese (0.6–0.8 Mn/0.4–0.2 Zn) [21–23,25,29] produces the particles with the best performance in terms of particle size, Ms and heating production by magnetic hyperthermia.

2.2. Thermal Decomposition Method

Highly monodispersed nanoparticles can be synthesized via thermal decomposition of organometallic precursors method. Through this method, organic iron compounds, such as ferric acetylacetonate or iron oleate, are decomposed at a high temperature inside the non-polar boiling solvent in the presence of capping agents [30]. The precursors are heated to the solvent boiling point at a constant heating rate and are kept at this temperature for the desired time. The nanoparticles are finally coated with a capping ligand, which is not only the colloidal stabilizer of the suspension but also an important tool to control the size and the shape of the crystals. Nanoparticles prepared by this technique are hydrophobic and can be stored in hexane, cyclohexane, toluene or other non-polar solvents [5]. Generally, the method produces high-quality nanoparticles. One of the most significant difficulties of this route is to establish a constant heating rate, especially in the range where the nucleation and growth occurs, and the production of a large-scale amount of nanomaterial.

In general, Mn-Zn ferrite nanoparticles were obtained by partially replacing the iron precursor ($Fe(acac)_3$) with the respective manganese and zinc acetylacetonates, in different proportions, in the typical protocol used for the synthesis of iron oxide nanoparticles. This method produces very regular particles with accurate control over the size distribution [31–33]. It has been observed that the introduction of doping elements (Mn and Zn) is more difficult in this method, with detected values significantly lower than the theoretical/expected ones [31,32]. This implies, in the X-ray diffraction (XRD) analysis of the obtained crystals, the presence of the pure magnetite-based phase. The magnetic characterizations of these nanoparticles reveal that, in fact, zinc is the element that is more responsible for the increase in Ms and SAR values, while the contribution of manganese is slightly negligible [32], partially in contrast with the analyses of nanoparticles obtained by co-precipitation.

2.3. Microemulsion Method

The microemulsion method uses water droplets as nanoreactors in a continuous phase (oil) in the presence of surfactant molecules. Nanoparticles with a controlled size are obtained by the simple mixing of two water-in-oil microemulsions: one containing a salt or a complex of metal and the other containing a reducing agent [34]. The microdroplets will continuously collide, coalesce, and break again, and, finally, produce a precipitate which is finally separated by extraction with polar solvents. Due to their small size, the droplets are subject to Brownian motion resulting in the formation of dimers and other aggregates with a short life, which rapidly disintegrate into droplets of the original size. The main drawback of this method concerns the inefficient scale-up, with lower yields of SPIONs compared to other techniques and the large volume of solvents necessary for the synthesis of significant amounts of magnetic material.

Makovec et al. reported the synthesis of Mn-Zn ferrite nanoparticles by inducing the co-precipitation of hydroxides of Mn, Zn and Fe ions in a microemulsion system, consisting of an aqueous phase, n-hexanol as the oil phase, and cetyltrimethylammonium bromide (CTAB) as the surfactant. By this method, the authors obtained $Mn_{0.5}Zn_{0.5}Fe_2O_4$ spinel-ferrite nanoparticles with a size ranging from 2 to 15 nm. Moreover, the distribution of the cations over the two sublattices of the spinel structure of the nanoparticles was deeply investigated in comparison to the bulk standard [35].

2.4. Hydrothermal Method

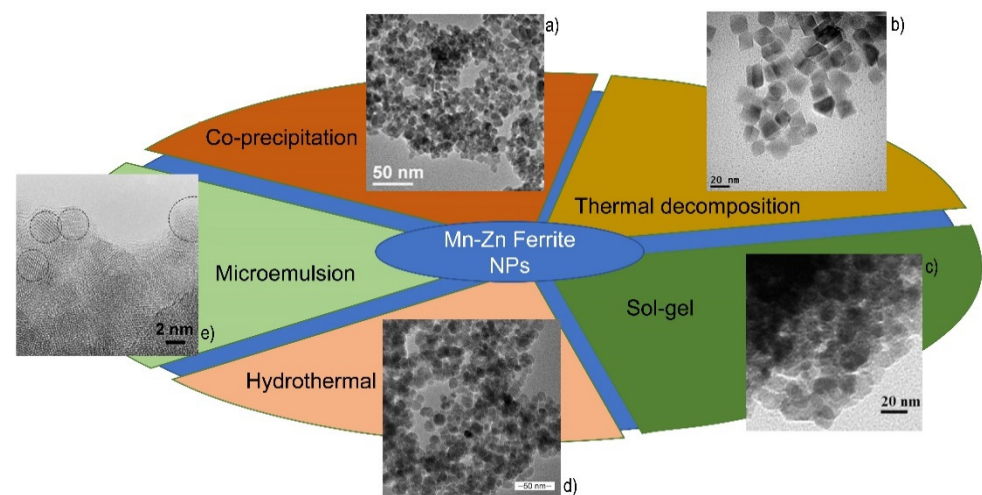
The hydrothermal process is one of the most promising synthesis methods which exploits the solubility of inorganic materials in water at elevated temperatures and pressures, with a resulting production of high-quality nanoparticles with controlled size and size distribution.

The first pioneering article on the synthesis of Mn-Zn ferrites was published in 1999 using the hydrothermal method, to apply the advances in research on this soft material, which is used mostly in electronics, to the biomedical field [36]. In more recent contributions, monophase Mn-Zn ferrite NPs, with a mean particle size of 7 nm, is used in the presence of citric acid as chelator. Interestingly, the capping agent was not only useful to disperse the nanoparticles by avoiding the aggregation between the cores, but its role was fundamental in increasing the crystal purity of the final nanoparticles, achieving, in addition, a control on the particle growth [37]. Similar evidence was observed by using another capping agent, the oleic acid, in the hydrothermal process. In this case, a significant reduction of the $\text{Mn}_{0.8}\text{Zn}_{0.2}\text{Fe}_2\text{O}_4$ crystal size in the presence of the surfactant was observed [38].

2.5. Sol-Gel Method

In the sol-gel method, a colloidal suspension of solids undergoes a process towards hydrolysis and condensation polymerization reactions to form a gel phase. In a typical reaction, the precursor is dispersed in a host liquid either by shaking, stirring or sonication, and the resultant system contains a liquid and a solid phase. Phase separation is carried out to recover the nanoparticles by various methods, such as sedimentation, filtration and centrifugation and the moisture is further removed by drying. Usually, the sol-gel method can be used for the preparation of a variety of ferrite nanoparticles in the stated temperature range. Typically, a citrate-gel is used as a template for the synthesis. The control of some parameters is crucial to obtain monophase Mn-Zn ferrite nanoparticles, as the pH of the precursor solution, the temperature of the process and the stoichiometry of the ferrite. Additionally, in this case, the best nanoparticles were observed with a Mn/Zn ratio between 1 and 1.5 [39,40].

Scheme 1 summarizes all the reported synthetic methods, with some representative TEM images of obtained nanoparticles.



Scheme 1. Schematic figure of the synthetic methods described for the preparation of Mn-Zn Ferrite nanoparticles for biomedical applications. Adapted with permission from (a): [20]; (b): [31]; (c): [40]; (d): [38]; (e): [35].

3. In Vitro Applications of Mn-Zn Ferrites

In this section, some recent studies, in which manganese-zinc ferrite nanoparticles have been tested within in vitro experiments, are analyzed. In the selection of relevant

contributions, some aspects were considered, such as the effective enhancement of the magnetic properties (e.g., magnetic saturation or r_2 relaxivity or SAR value), that justified the use of a doped ferrite in alternative to bare iron oxide nanoparticles, and the application of these nanoparticles in an in vitro assay, with particular consideration of the biocompatibility of the nanomaterial.

Qu et al. presented a study on the synthesis of $Mn_xZn_{1-x}Fe_2O_4$ ferrite nanoparticles with a size of around 8 nm. For these nanoparticles, obtained by thermal decomposition, the ratio between Zn and Mn was inversely varied, finding $Mn_{0.6}Zn_{0.4}Fe_2O_4$ as the best composition in terms of M_s (76.7 emu/g). These nanoparticles were then transferred in the aqueous phase through the use of a synthetic amphiphilic block copolymer obtained from mPEG and poly(caprolactone) (PEG-PLC), obtaining ultra-stable clusters of about 100–150 nm. The size of these clusters and their magnetization were modulated by varying the mass ratios between the particles and polymer. In terms of magnetic hyperthermia, however, it was noted that the ferrites obtained with Mn only show a higher SAR (1618 W/g) than $Mn_{0.6}Zn_{0.4}Fe_2O_4$ (1100 W/g). From the experiments conducted on MCF-7 and drug-resistant MCF-7/ADR cancer cells in vitro, it can be seen that the application of magnetic hyperthermia generated high levels of cellular depletion of up to 90% within 15 min, obtained mainly by induction of apoptotic and non-necrotic phenomena [41].

In addition, in the work of Guo et al. the Mn-Zn ferrite nanoparticles were synthesized by thermal decomposition, obtaining monodisperse nanoparticles of 10 nm, with a quasi-cubic morphology. In addition to a good r_2 relaxivity and an excellent biocompatibility (with cytotoxicity of 10% at the highest tested concentration and a hemolysis rate of 1.12%), these ferrites showed a very high magnetic saturation, equal to 98 emu/g. These nanoparticles were then investigated as a potential actuator for magnetic hyperthermia, obtaining an increase in temperature of up to 42–44 °C within 20 min, at 235 kHz, with a particularly low concentration of 60 µg/mL. In addition, the nanoparticles were evaluated as carriers for gene therapy, assessing the ability to transfect CD44-shRNA-EGFP plasmids into the ovarian cancer SK-OV-3 cells, obtaining a transfection efficiency of 58%, which is comparable to the standard liposome method [42].

Applying a different synthetic method, Sobhani et al. reported the preparation of manganese-zinc ferrite nanoparticles that were obtained by a hydrothermal route, obtaining particles with a TEM diameter of approximately 14 nm and a hydrodynamic diameter of approximately 400 nm. These particles, stabilized with a PEG outer layer, showed a higher relaxivity r_2 , 85 $mM^{-1} s^{-1}$ compared to the commercial equivalent (Sinerem). Taking into account a low-mild cytotoxicity, two different cell lineages, 4T1 and L929 cells, were incubated and then analyzed by MRI to evaluate the T_2 signal decrease, obtaining a decrease of signal intensity in T_2 -weighted images, of 25% at an iron concentration of 0.4 mg/mL and 45% at a concentration of 0.8 mg/mL [43].

4. In Vivo Applications of Mn-Zn Ferrites

In this section, the studies that exploited manganese-zinc ferrites nanoparticles into in vivo experiments will be analyzed. For the medical validation of this quite novel nanomaterial, the administration in a living system is very important, because many results concerning magnetic nanoparticles, fully demonstrated in solution or by in vitro experiments, were not reproduced in vivo. As in the previous section, the analysis is focused on those papers that provided real advancement in the medical usage of Mn-Zn ferrite nanoparticles. It should be noted that all these studies have been published in the last six years, reflecting the very recent development of the medical application of these ferrites.

In 2015, Leng et al. reported the preparation of hydrophobic spherical $Mn_{0.6}Zn_{0.4}Fe_2O_4$ nanocrystals, with an average diameter of 8 nm, and a star-shaped copolymer 4sPCL-*b*-P(MEO₂MA-*co*-OEGMA), starting from the in vitro study reported in [41], described in Section 3. The magnetic nanoparticles, obtained by a standard thermal decomposition method, were then resuspended in THF with the polymer and quite small nanoclusters

were obtained, with an average size of 122 nm. These composites showed low toxicity, by *in vitro* assay, and a relevant r_2 of $138 \text{ mM}^{-1} \text{ s}^{-1}$ at 3.0 T. For assessing the MRI potential of the system, the magnetic micelles were intravenously injected in mice that were bearing a xenograft tumor at a low dose of 0.007 mmol Fe/kg . By MRI, a significant darkening of the tumor region was observed after 1 h in T_2 -weighted spin-echo analyses, with a maximum signal recorded at 4 h. At 8 h after injection, the signal in the tumor region recovered the contrast level of pre-injection imaging [41,44].

Herynek et al. presented the synthesis of superparamagnetic silica-coated small nanoclusters of Mn-Zn ferrite nanoparticles. In this structure, few nanoparticles represent the magnetic core (about 30 nm) entrapped in silica beads with an overall size of 80–100 nm. Interestingly, the r_2 relaxivity reached $295 \text{ mM}^{-1} \text{ s}^{-1}$ at 0.5 T, which is approximately two times higher than commercial analogs of Resovist. Within this framework, some bioluminescent cells from the adipose tissue were labeled with the silica-coated nanoparticles and were grafted into rat muscle, in order to monitor the signal in a long-term experiment. The bioluminescent signal was revealed after one day, but after a week the luminescence decreased at 10%. On the opposite, the MRI signal recorded by T_2/T_2^* images was detected from day 1 to day 28 without visible change [45].

Another assembly of hydrophobic $\text{Mn}_{0.63}\text{Zn}_{0.37}\text{Fe}_2\text{O}_4$ nanoparticles in dense spherical clusters or in small chains of few crystals, namely worm-like clusters, was reported by Sun et al. The three different configurations offered quite different MRI profiles at 1.5 T, with r_2 values ranging from $237 \text{ mM}^{-1} \text{ s}^{-1}$ for single nanoparticles, to $318 \text{ mM}^{-1} \text{ s}^{-1}$ for spherical clusters and $474 \text{ mM}^{-1} \text{ s}^{-1}$ for the worm-like chains. The trend was also observed for the magnetization values of the three nanosystems, with the worm-like cluster showing the higher saturation, slightly higher even than the hydrophobic Mn-Zn ferrite nanoparticles. Moreover, the nanosystems were transferred in water by means of a modified polymer, in which an arginylglycylaspartic acid moiety (RGD) was included to target the integrin $\alpha v \beta 3$ that is overexpressed in HUVEC endothelial cells. No relevant differences were observed by *in vitro* test, but the MRI analysis after intravenous administration revealed that the worm-like structure induced a higher penetration in the tumor region. The author hypothesized a model in which the elongated structure has more chance to interact with cellular receptor in the fluid environment, therefore forming the receptor-mediated endocytosis more easily [46].

Albarqi et al. recently proposed the preparation of small nanoclusters for the therapy of prostatic cancer. Iron oxide nanoparticles doped with zinc and manganese, with a size of 13 nm, were obtained by the thermal decomposition of $\text{Fe}(\text{acac})_3$, ZnCl_2 and MnCl_2 . These hydrophobic nanoparticles were subsequently transferred in water using the solvent evaporation method, adding PEG-PCL as template for the preparation of very small clusters of 100 nm. As expected, the doped nanoparticles were characterized by a higher saturation magnetization value ($60.33 \text{ Am}^2/\text{kg}$) than iron oxide nanoparticles ($57 \text{ Am}^2/\text{kg}$). Moreover, the SAR values (measured in THF at 420 kHz, 26.9 kA/m) were improved for doped nanoparticles (1615.1 W/g) if compared to bare iron oxide nanoparticles (586.2 W/g). When the nanoparticles were clustered and transferred in water, a slight decrease of SAR values was observed, but, regardless, the Mn-Zn magnetic cluster showed a higher performance (1010.0 W/g) than the iron oxide nanoclusters (493.8 W/g). The clusters were intravenously administrated to some nude mice bearing subcutaneous xenografts of DU145 prostate cancer cells. The particles started to accumulate in the tumor site (via passive targeting) after 1 h and reached a maximum concentration after 7 h, with a minor accumulation in other organs (Figure 1A). The application of AFM to the animal induced an intertumoral temperature of 42°C and an evident inhibition of the tumor growth, also in comparison to the bare iron oxide clusters (Figure 1B) [47].

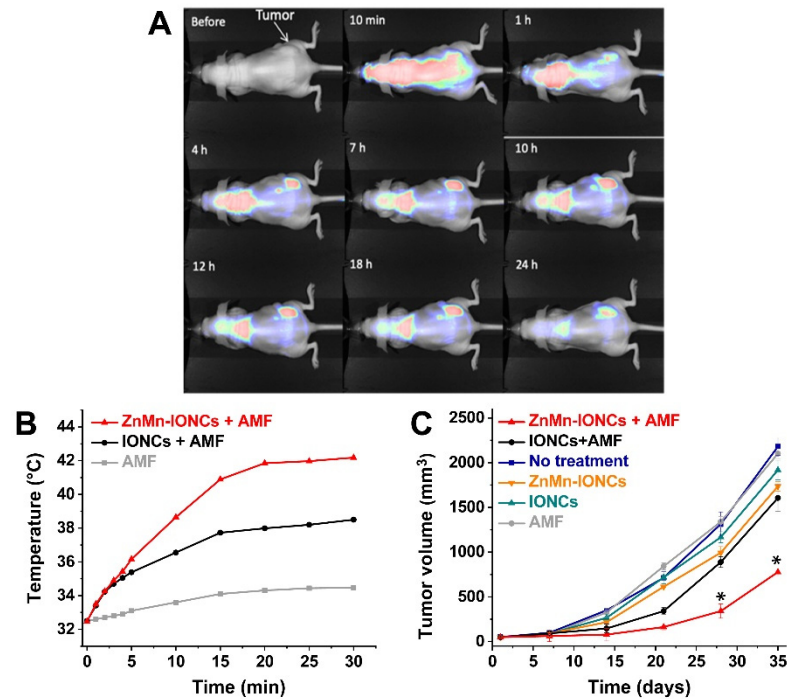


Figure 1. (A) NIR fluorescence images of a mouse at different time points following intravenous administration of the Mn-Zn magnetic cluster. (B,C) Intratumoral temperature curves during AFM and corresponding tumor growth profiles for each experimental group. Adapted with permission from [47], MDPI, 2020.

Wang et al. started from hydrophobic $Mn_{0.6}Zn_{0.4}Fe_2O_4$ nanoparticles for the preparation of magnetic PEG-*b*-PCL block copolymer micelles. The surface of the magnetic cluster was then engineered with hyaluronic acid (HA) for the active targeting of tumor cells, such as A549 (human lung adenocarcinoma cell line), over-expressing the receptor (CD44) for the HA. The purpose of this approach was to combine a magnetic hyperthermia therapeutic approach with radiotherapy for the treatment of non-small-cell lung cancer (Figure 2). By the in vitro test, a synergistic effect of the dual therapy was observed, with a total apoptosis rate of 32.7%, almost four times that of the results of hyperthermia and five times for radiotherapy. The synergistic effect was obtained also by in vivo treatment of xenograft tumor in mice. The nanocomposite was injected by tail vein in the animal and the therapeutic scheme was applied on days 1 and 4. The growth of the tumor appeared to be significantly inhibited with the relative tumor volume ratio shrinking to 49.6% by day 13 in the dual therapy group [48].

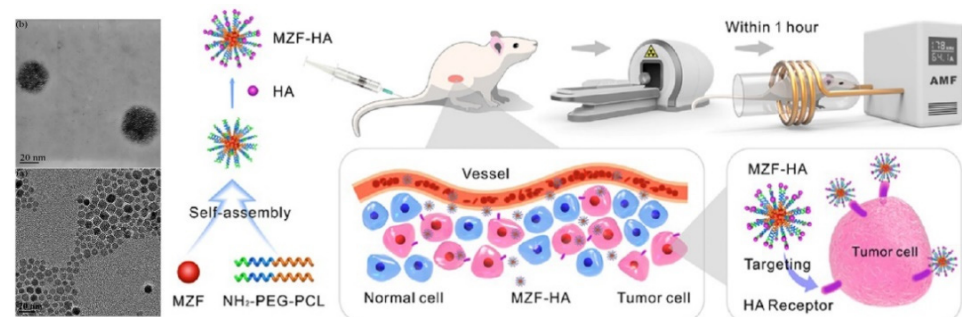


Figure 2. Scheme of the application of the Mn-Zn ferrite nanoclusters in an in vivo AFM experiment. On the left, TEM images of single nanoparticles (bottom) and clustered ones (top). Adapted with permission from [48], Copyright 2020, American Chemical Society.

5. Perspectives

The editorial contributions that promoted the use of magnetic nanoparticles doped with zinc and manganese ($Mn_xZn_{1-x}Fe_2O_4$) for application in the biomedical field have been mainly published in the last 10 years. This material has several peculiarities, in terms of magnetic characteristics, for application in diagnostics (e.g., by MRI) or even as an actuator agent in magnetic hyperthermia, showing higher SAR levels than the respective iron oxide nanoparticles. The main concern of the use of this material could lie in its possible toxicity, but the studies reported in this review did not report acute events or a cytotoxicity different from that which can usually be observed for iron oxide-based magnetic nanoparticles. It should also be considered that the release of metal ions, due to the normal in vivo degradation of the nanoparticles, is a slow process; therefore, the adverse effects due to the leakage of zinc and manganese are negligible. Certainly, the use of the nanoparticle is subject to a general assessment of the risks due to the administration of a nanomaterial, due to its size and clearance from the organism, which for Mn-Zn ferrite nanoparticles could be considered as comparable to that of iron oxide nanoparticles. The use of ferrites is, however, still at a low Technology Readiness Level (TRL). Thus, to the best of our knowledge, no formulations are still approved for clinical use in humans. Furthermore, the improved magnetic properties could also help to decrease the amount of particles used in the medical application, with fewer side effects due to the introduction of inorganic nanomaterial in a living system. The few studies that reached the stage of therapeutic exploitation on small animals confirmed the high potential of this nanomaterial. Certainly, there are still several aspects to investigate, especially at the level of the control of the elemental composition of the nanoparticle, since different doping percentages produce drastic changes in the magnetic properties of the material. This elemental control is also different according to the selected synthetic method. Therefore, in the design of an experiment involving the use of these nanoparticles, fine control over the final stoichiometry of the material, and over the magnetic properties, becomes fundamental.

Author Contributions: Conceptualization, R.D.C.; writing—original draft preparation, R.D.C. and L.M.S.; writing—review and editing, R.D.C. and R.R. All authors have read and agreed to the published version of the manuscript.

Funding: This research was funded by BIO-D project (ARS01_00876) co-financed by European Union—ERDF—ESF—PON Research and Innovation 2014–2020 and by Italian PON “Dottorati Innovativi a Caratterizzazione Industriale” (project n°1 DOT1312457).

Institutional Review Board Statement: Not applicable.

Informed Consent Statement: Not applicable.

Conflicts of Interest: The authors declare no conflict of interest.

References

1. Doane, T.L.; Burda, C. The unique role of nanoparticles in nanomedicine: Imaging, drug delivery and therapy. *Chem. Soc. Rev.* **2012**, *41*, 2885–2911. [[CrossRef](#)]
2. Wong, X.Y.; Sena-Torralba, A.; Alvarez-Diduk, R.; Muthoosamy, K.; Merkoci, A. Nanomaterials for nanotheranostics: Tuning their properties according to disease needs. *ACS Nano* **2020**, *14*, 2585–2627. [[CrossRef](#)]
3. Lin, X.M.; Samia, A.C.S. Synthesis, assembly and physical properties of magnetic nanoparticles. *J. Magn. Magn. Mater.* **2006**, *305*, 100–109. [[CrossRef](#)]
4. Zhang, Y.; Kohler, N.; Zhang, M.Q. Surface modification of superparamagnetic magnetite nanoparticles and their intracellular uptake. *Biomaterials* **2002**, *23*, 1553–1561. [[CrossRef](#)]
5. Figuerola, A.; Di Corato, R.; Manna, L.; Pellegrino, T. From iron oxide nanoparticles towards advanced iron-based inorganic materials designed for biomedical applications. *Pharmacol. Res.* **2010**, *62*, 126–143. [[CrossRef](#)]
6. Gobbo, O.L.; Sjaastad, K.; Radomski, M.W.; Volkov, Y.; Prina-Mello, A. Magnetic nanoparticles in cancer theranostics. *Theranostics* **2015**, *5*, 1249–1263. [[CrossRef](#)] [[PubMed](#)]
7. Dadfar, S.M.; Roemhild, K.; Drude, N.I.; von Stillfried, S.; Knuchel, R.; Kiessling, F.; Lammers, T. Iron oxide nanoparticles: Diagnostic, therapeutic and theranostic applications. *Adv. Drug Deliv. Rev.* **2019**, *138*, 302–325. [[CrossRef](#)] [[PubMed](#)]

8. Doaga, A.; Cojocariu, A.M.; Amin, W.; Heib, F.; Bender, P.; Hempelmann, R.; Caltun, O.F. Synthesis and characterizations of manganese ferrites for hyperthermia applications. *Mater. Chem. Phys.* **2013**, *143*, 305–310. [[CrossRef](#)]
9. Andersen, H.L.; Saura-Muzquiz, M.; Granados-Miralles, C.; Canevet, E.; Lock, N.; Christensen, M. Crystalline and magnetic structure-property relationship in spinel ferrite nanoparticles. *Nanoscale* **2018**, *10*, 14902–14914. [[CrossRef](#)]
10. Gazeau, F.; Levy, M.; Wilhelm, C. Optimizing magnetic nanoparticle design for nanothermotherapy. *Nanomedicine* **2008**, *3*, 831–844. [[CrossRef](#)]
11. Bante-Guerra, J.; Macias, J.D.; Caballero-Aguilar, L.; Vales-Pinzon, C.; Alvarado-Gil, J.J. Infrared thermography analysis of thermal diffusion induced by RF magnetic field on agar phantoms loaded with magnetic nanoparticles. In Proceedings of the SPIE Conference on Energy-Based Treatment of Tissue and Assessment VII, San Francisco, CA, USA, 3–4 February 2013.
12. Jang, J.T.; Nah, H.; Lee, J.H.; Moon, S.H.; Kim, M.G.; Cheon, J. Critical enhancements of MRI contrast and hyperthermic effects by dopant-controlled magnetic nanoparticles. *Angew. Chem. Int. Ed.* **2009**, *48*, 1234–1238. [[CrossRef](#)]
13. Lee, J.H.; Huh, Y.M.; Jun, Y.; Seo, J.; Jang, J.; Song, H.T.; Kim, S.; Cho, E.J.; Yoon, H.G.; Suh, J.S.; et al. Artificially engineered magnetic nanoparticles for ultra-sensitive molecular imaging. *Nat. Med.* **2006**, *13*, 95–99. [[CrossRef](#)]
14. Thakur, P.; Chahar, D.; Taneja, S.; Bhalla, N.; Thakur, A. A review on MnZn ferrites: Synthesis, characterization and applications. *Ceram. Int.* **2020**, *46*, 15740–15763. [[CrossRef](#)]
15. Massart, R. Preparation of aqueous magnetic liquids in alkaline and acidic media. *IEEE Trans. Magn.* **1981**, *17*, 1247–1248. [[CrossRef](#)]
16. Sun, T.; Borrasso, A.; Liu, B.; Dravid, V. Synthesis and Characterization of nanocrystalline zinc manganese ferrite. *J. Am. Ceram. Soc.* **2011**, *94*, 1490–1495. [[CrossRef](#)]
17. Sugimoto, M. The past, present, and future of ferrites. *J. Am. Ceram. Soc.* **2004**, *82*, 269–280. [[CrossRef](#)]
18. Lu, A.-H.; Salabas, E.L.; Schueth, F. Magnetic nanoparticles: Synthesis, protection, functionalization, and application. *Angew. Chem. Int. Ed.* **2007**, *46*, 1222–1244. [[CrossRef](#)]
19. Babes, L.; Denizot, B.; Tanguy, G.; Le Jeune, J.J.; Jallet, P. Synthesis of iron oxide nanoparticles used as MRI contrast agents: A parametric study. *J. Colloid Interface Sci.* **1999**, *212*, 474–482. [[CrossRef](#)]
20. De Mello, L.B.; Varanda, L.C.; Sigoli, F.A.; Mazali, I.O. Co-precipitation synthesis of (Zn-Mn)-co-doped magnetite nanoparticles and their application in magnetic hyperthermia. *J. Alloys Compd.* **2018**, *779*, 698–705. [[CrossRef](#)]
21. Veena Gopalan, E.; Al-Omari, I.A.; Malini, K.A.; Joy, P.A.; Sakthi Kumar, D.; Yoshida, Y.; Anantharaman, M.R. Impact of zinc substitution on the structural and magnetic properties of chemically derived nanosized manganese zinc mixed ferrites. *J. Magn. Magn. Mater.* **2008**, *321*, 1092–1099. [[CrossRef](#)]
22. Kareem, S.H.; Ati, A.A.; Shamsuddin, M.; Lee, S.L. Nanostructural, morphological and magnetic studies of PEG/Mn(1-x)Zn(x)Fe₂O₄ nanoparticles synthesized by co-precipitation. *Ceram. Int.* **2015**, *41*, 11702–11709. [[CrossRef](#)]
23. Nasrin, S.; Chowdhury, F.U.Z.; Hoque, S.M. Study of hydrodynamic size distribution and hyperthermia temperature of chitosan encapsulated zinc-substituted manganese nano ferrites suspension. *Phys. B Condens. Matter* **2019**, *561*, 54–63. [[CrossRef](#)]
24. Patade, S.R.; Andhare, D.D.; Khedkar, M.V.; Jadhav, S.A.; Jadhav, K.M. Synthesis and characterizations of magnetically inductive Mn-Zn spinel ferrite nanoparticles for hyperthermia applications. *J. Mater. Sci. Mater. Electron.* **2021**, *32*, 13685–13692. [[CrossRef](#)]
25. Latorre-Esteves, M.; Cortés, A.; Torres-Lugo, M.; Rinaldi, C. Synthesis and characterization of carboxymethyl dextran-coated Mn/Zn ferrite for biomedical applications. *J. Magn. Magn. Mater.* **2009**, *321*, 3061–3066. [[CrossRef](#)]
26. Salehpour, F.; Khorramdin, A.; Shokrollahi, H.; Pezeshki, A.; Mirzaei, F.; Nader, N.D. Synthesis of Zn-doped manganese ferrite nanoparticles via coprecipitation method for magnetic resonance imaging contrast agent. *J. Nanotechnol. Eng. Med.* **2014**, *5*, 041002. [[CrossRef](#)]
27. Raland, R.D.; Borah, J.P. Efficacy of heat generation in CTAB coated Mn doped ZnFe₂O₄ nanoparticles for magnetic hyperthermia. *J. Phys. D Appl. Phys.* **2016**, *50*, 035001. [[CrossRef](#)]
28. Arulmurugan, R.; Jeyadevan, B.; Vaidyanathan, G.; Sendhilnathan, S. Effect of zinc substitution on Co-Zn and Mn-Zn ferrite nanoparticles prepared by co-precipitation. *J. Magn. Magn. Mater.* **2004**, *288*, 470–477. [[CrossRef](#)]
29. Hejase, H.; Hayek, S.S.; Qadri, S.; Haik, Y. MnZnFe nanoparticles for self-controlled magnetic hyperthermia. *J. Magn. Magn. Mater.* **2012**, *324*, 3620–3628. [[CrossRef](#)]
30. Zeng, H.; Rice, P.M.; Wang, S.X.; Sun, S. Shape-Controlled synthesis and shape-induced texture of MnFe₂O₄ nanoparticles. *J. Am. Chem. Soc.* **2004**, *126*, 11458–11459. [[CrossRef](#)]
31. Orsini, N.J.; Milic, M.M.; Torres, T.E. Zn- and (Mn, Zn)-substituted versus unsubstituted magnetite nanoparticles: Structural, magnetic and hyperthermic properties. *Nanotechnology* **2020**, *31*, 225707. [[CrossRef](#)]
32. Pardo, A.; Pelaz, B.; Gallo, J.; Bañobre-López, M.; Parak, W.J.; Barbosa, S.; del Pino, P.; Taboada, P. Synthesis, characterization, and evaluation of superparamagnetic doped ferrites as potential therapeutic nanotools. *Chem. Mater.* **2020**, *32*, 2220–2231. [[CrossRef](#)]
33. Jeun, M.; Moon, S.J.; Kobayashi, H.; Shin, H.Y.; Tomitaka, A.; Kim, Y.J.; Takemura, Y.; Paek, S.H.; Park, K.H.; Chung, K.-W.; et al. Effects of Mn concentration on the ac magnetically induced heating characteristics of superparamagnetic Mn_xZn_{1-x}Fe₂O₄ nanoparticles for hyperthermia. *Appl. Phys. Lett.* **2010**, *96*, 202511. [[CrossRef](#)]
34. Muller, B.W.; Muller, R.H. Particle size distributions and particle size alterations in microemulsions. *J. Pharm. Sci.* **1984**, *73*, 919–922. [[CrossRef](#)] [[PubMed](#)]

35. Makovec, D.; Kodre, A.; Arčon, I.; Drogenik, M. Structure of manganese zinc ferrite spinel nanoparticles prepared with co-precipitation in reversed microemulsions. *J. Nanoparticle Res.* **2008**, *11*, 1145–1158. [[CrossRef](#)]
36. Rath, C.; Sahu, K.K.; Anand, S.; Date, S.K.; Mishra, N.C.; Das, R.P. Preparation and characterization of nanosize Mn-Zn ferrite. *Magn. Magn. Mater.* **1999**, *202*, 77–84. [[CrossRef](#)]
37. Zahraei, M.; Monshi, A.; Morales, M.D.; Shahbazi-Gahrouei, D.; Amirnasr, M.; Behdadfar, B. Hydrothermal synthesis of fine stabilized superparamagnetic nanoparticles of Zn²⁺ substituted manganese ferrite. *J. Magn. Magn. Mater.* **2015**, *393*, 429–436. [[CrossRef](#)]
38. Kaewmanee, T.; Wannapop, S.; Phuruangrat, A.; Thongtem, T.; Wiranwetchayan, O.; Promnopas, W.; Sansongsiri, S.; Thongtem, S. Effect of oleic acid content on manganese-zinc ferrite properties. *Inorg. Chem. Commun.* **2019**, *103*, 87–92. [[CrossRef](#)]
39. Seyyed Ebrahimi, S.A.; Masoudpanah, S.M. Effects of pH and citric acid content on the structure and magnetic properties of MnZn ferrite nanoparticles synthesized by a sol–gel autocombustion method. *J. Magn. Magn. Mater.* **2014**, *357*, 77–81. [[CrossRef](#)]
40. Thota, S.; Kashyap, S.C.; Sharma, S.K.; Reddy, V.R. Micro Raman, Mossbauer and magnetic studies of manganese substituted zinc ferrite nanoparticles: Role of Mn. *J. Phys. Chem. Solids* **2016**, *91*, 136–144. [[CrossRef](#)]
41. Qu, Y.; Li, J.; Ren, J.; Leng, J.; Lin, C.; Shi, D. Enhanced magnetic fluid hyperthermia by micellar magnetic nanoclusters composed of Mn_xZn_{1-x}Fe₂O₄ nanoparticles for induced tumor cell apoptosis. *ACS Appl. Mater. Interfaces* **2014**, *6*, 16867–16879. [[CrossRef](#)]
42. Guo, T.; Dou, F.; Lin, M.; Huang, J.; Zhou, C.; Zhang, J.; Yu, H.; Jiang, X.; Ye, J.; Shi, Y.; et al. Biological characteristics and carrier functions of pegylated manganese zinc ferrite nanoparticles. *J. Nanomater.* **2019**, *2019*, 1–10. [[CrossRef](#)]
43. Sobhani, T.; Shahbazi-Gahrouei, D.; Rostami, M.; Zahraei, M.; Farzadniya, A. Assessment of manganese-zinc ferrite nanoparticles as a novel magnetic resonance imaging contrast agent for the detection of 4T1 breast cancer cells. *Med. Signals Sens.* **2019**, *9*, 245–251. [[CrossRef](#)]
44. Leng, J.; Li, J.; Ren, J.; Deng, L.; Lin, C. Star–block copolymer micellar nanocomposites with Mn, Zn-doped nano-ferrite as superparamagnetic MRI contrast agent for tumor imaging. *Mater. Lett.* **2015**, *152*, 185–188. [[CrossRef](#)]
45. Herynek, V.; Turnovcova, K.; Galisova, A.; Kaman, O.; Marekova, D.; Koktan, J.; Vosmanska, M.; Kosinova, L.; Jendelova, P. Manganese-zinc ferrites: Safe and efficient nanolabels for cell imaging and tracking in vivo. *ChemistryOpen* **2019**, *8*, 155–165. [[CrossRef](#)]
46. Sun, Y.; Yan, C.; Xie, J.; Yan, D.; Hu, K.; Huang, S.; Liu, J.; Zhang, Y.; Gu, N.; Xiong, F. High-Performance Worm-like Mn-Zn Ferrite Theranostic Nanoagents and the Application on Tumor Theranostics. *ACS Appl. Mater. Interfaces* **2019**, *11*, 29536–29548. [[CrossRef](#)] [[PubMed](#)]
47. Albarqi, H.A.; Demessie, A.A.; Sabei, F.Y.; Moses, A.S.; Hansen, M.N.; Dhagat, P.; Taratula, O.R.; Taratula, O. Systemically Delivered Magnetic Hyperthermia for Prostate Cancer Treatment. *Pharmaceutics* **2020**, *12*, 1020. [[CrossRef](#)]
48. Wang, Y.; Zou, L.; Qiang, Z.; Jiang, J.; Zhu, Z.; Ren, J. Enhancing targeted cancer treatment by combining hyperthermia and radiotherapy using Mn-Zn ferrite magnetic nanoparticles. *ACS Biomater. Sci. Eng.* **2020**, *6*, 3550–3562. [[CrossRef](#)]